Rhodium doped manganites: Ferromagnetism and metallicity

Raveau, B.; Hebert, S.; Maignan, A.; Fresard, R.; Hervieu, M.; Khomskii, D. I.

Published in:
Journal of Applied Physics

DOI:
10.1063/1.1380412

Publication date:
2001

Rhodium doped manganites: Ferromagnetism and metallicity

B. Raveau, S. Hébert, A. Maignan, R. Frésard, M. Hervieu, and D. Khomskii

Citation: Journal of Applied Physics **90**, 1297 (2001); doi: 10.1063/1.1380412
View online: https://doi.org/10.1063/1.1380412
View Table of Contents: http://aip.scitation.org/toc/jap/90/3
Published by the American Institute of Physics

Rhodium doped manganites: Ferromagnetism and metallicity

B. Raveau, S. Hébert,[a] A. Maignan, R. Frésard, and M. Hervieu
Laboratoire Crismat, Ismra, 6 Boulevard du Maréchal Juin, 14050 Caen Cedex, France

D. Khomskii
Solid State Physics Laboratory, Materials Science Centre, University of Groningen, Nijenborgh 4, 9747 A6 Groningen, The Netherlands

(Received 14 March 2001; accepted for publication 23 April 2001)

It is shown that ferromagnetism and insulator to metal transitions in small *A* site cation manganites $Pr_{1-x}Ca_xMnO_3$ are induced by rhodium doping. Colossal magnetoresistance properties are evidenced for a large compositional range ($0.35 \leqslant x < 0.60$). The ability of rhodium to induce such properties is compared to the results obtained by chromium and ruthenium doping. Models are proposed to explain this behavior. © *2001 American Institute of Physics.*
[DOI: 10.1063/1.1380412]

I. INTRODUCTION

The perovskite manganites $Ln_{1-x}Ca_xMnO_3$ often exhibit, at low temperature, a charge ordered state,[1–6] whose metastable character is crucial for the appearance of colossal magnetoresistance (CMR). The CMR effect in these cases is indeed based on the competition between the insulating charge ordered state and the ferromagnetic metallic state that takes place when a magnetic field is applied, also leading to the phase separation phenomena.[7–13] In those manganites, the stability of the charge ordered (CO) state increases as the size of the *A*-site cation decreases[14–17] so that the possibility of obtaining a ferromagnetic metallic state under a magnetic field is hindered for small *A*-site cations, and consequently CMR, disappears.

An interesting route to induce CMR in such perovskites consists of doping Mn sites with foreign cations, since such a method weakens and even destroys the ordering of Mn^{3+} and Mn^{4+} species. Nevertheless, the collapse of CO is not sufficient to induce CMR, since it should also enhance ferromagnetism and metallicity. For this reason, only some magnetic cations, such as cobalt, nickel,[18] chromium,[19,20] and recently ruthenium,[21–24] were found to be effective dopants. Rhodium, because of its two stable electronic configurations, $Rh(III)$-d^6 and $Rh(IV)$-d^5 is a potential dopant for CMR manganites. We report herein on the possibility of inducing both ferromagnetism and metallicity in $Pr_{1-x}Ca_xMnO_3$ manganites by doping with rhodium. We show that the behavior of rhodium is rather similar to chromium, but with smaller Curie temperatures T_C and larger resistivities.

II. EXPERIMENT

The manganites $Ln_{1-x}Ca_xMn_{1-y}Rh_yO_3$ were synthesized from intimate mixtures of oxides Pr_6O_{11} or Sm_2O_3, CaO, Mn_2O_3 and Rh_2O_3 first heated in air at 1050 °C for 12 h, then sintered in the form of bars up to 1400 °C for 12 h and slowly cooled down to room temperature at 100 K h^{-1}. The magnetic measurements were performed with a superconducting quantum interference device magnetometer under 1.45 T, whereas the transport measurements were carried out with a Quantum Design physical properties measurements system, under 0 and 7 T (four-probe method). The purity of the samples was checked by electron diffraction (ED) using a 200 kV microscope, and the cationic composition was determined by energy dispersive spectroscopy, using a Kevex analyzer. The analyses carried out for numerous crystallites show an homogeneous distribution of the cations and an actual composition very close to the nominal one, within the limit of the technique accuracy. *T*-dependent ED and lattice imaging were also carried out between 92 and 400 K. Thermopower measurements were made under zero applied magnetic field using a four-point steady state method with separate measuring and power contacts. More details of the experimental setup are given in Ref. 25.

III. RESULTS

The rhodium substitution for manganese in the hole doped manganites $Pr_{0.8}Ca_{0.2}MnO_3$ and $Pr_{0.7}Ca_{0.3}MnO_3$ does not significantly influence the magnetic and transport properties of these compounds: these oxides remain insulators and ferromagnetic whatever the rhodium level up to 10% Rh, with a T_C taken at the inflection point close to 120 K to be compared to 120 K for the pristine compounds.[26] Similarly, the magnetic moment at 5 K for $Pr_{0.8}Ca_{0.2}MnO_3$, $M = 3.7\mu_B$ is not greatly affected, leading to $M = 3.2\mu_B$ for $Pr_{0.8}Ca_{0.2}Mn_{0.9}Rh_{0.1}O_3$. Nevertheless, the doping with rhodium significantly reinforces ferromagnetism as the calcium content increases, as shown for $Pr_{0.7}Ca_{0.3}MnO_3$, whose magnetic moment at 5 K, $M = 1.7\mu_B$ is increased to $M = 2.7\mu_B$ by doping with 5% Rh.

But the most spectacular effect appears for the manganites $Pr_{1-x}Ca_xMnO_3$ with $0.35 \leqslant x \leqslant 0.50$, for which the doping with rhodium induces a dramatic increase of ferromagnetism as illustrated by the $M(T)$ curves of $Pr_{0.65}Ca_{0.35}Mn_{1-y}Rh_yO_3$ [Fig. 1(a)] and of $Pr_{0.5}Ca_{0.5}Mn_{1-y}Rh_yO_3$ [Fig. 1(b)] which show that the mag-

[a]Author to whom correspondence should be addressed; electronic mail: sylvie.hebert@ismra.fr

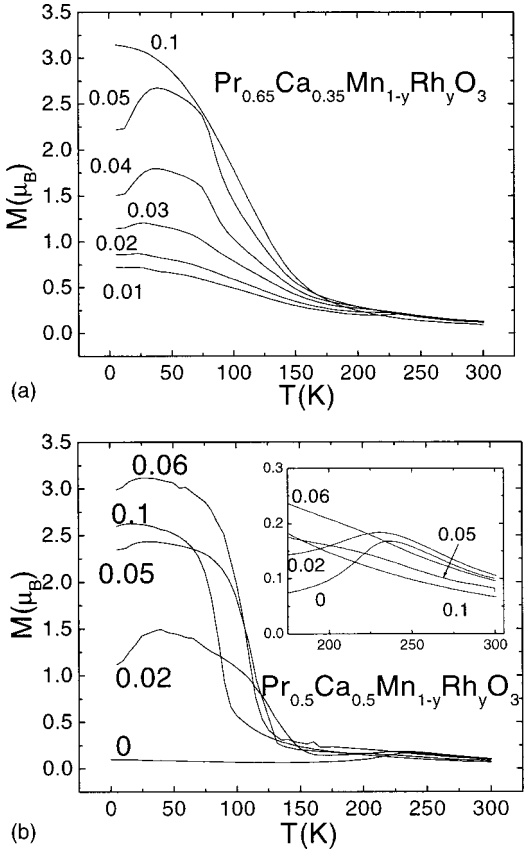

FIG. 1. T dependence of the magnetization M collected in 1.45 T after a zero field cooled process for the series: (a) $Pr_{0.65}Ca_{0.35}Mn_{1-y}Rh_yO_3$ and (b) $Pr_{0.5}Ca_{0.5}Mn_{1-y}Rh_yO_3$. y values are labeled in the graph. Inset of (b): enlargement in the vicinity of T_{CO}.

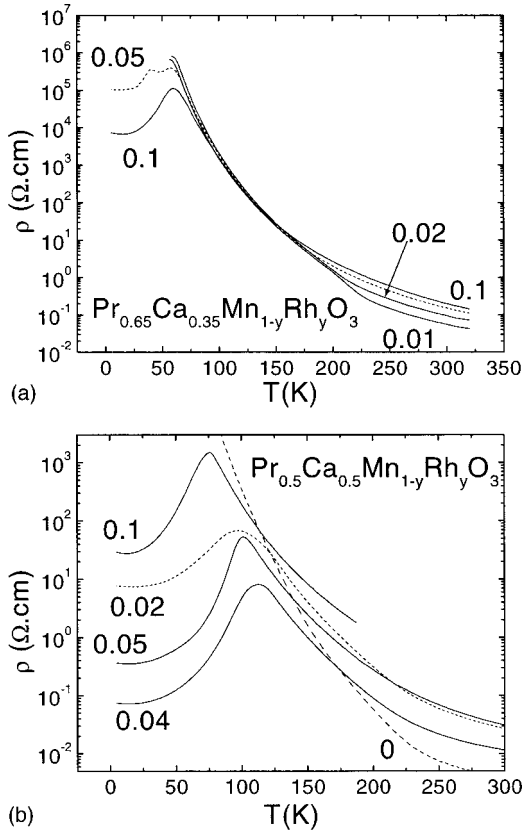

FIG. 2. T dependence of the resistivity ρ registered upon cooling from 400 K in the absence of magnetic field for the series: (a) $Pr_{0.65}Ca_{0.35}Mn_{1-y}Rh_yO_3$ and (b) $Pr_{0.5}Ca_{0.5}Mn_{1-y}Rh_yO_3$.

netic moment of the pristine oxide at 5 K, smaller than $0.5\mu_B$, is increased up to $3.2\mu_B$ by doping with rhodium. As shown for $Pr_{0.5}Ca_{0.5}Mn_{1-y}Rh_yO_3$, the magnetic moment generally increases regularly with the rhodium content reaching the magnitude close to the theoretical value ($\sim 3.5\mu_B$) for $y=0.06$ and then decreases again as y increases [Fig. 1(b)]. Concomitantly, the magnetization maximum at about 250 K, which is characteristic of the charge-ordering setting in $Pr_{0.5}Ca_{0.5}MnO_3$, tends to disappear as the Rh content increases and is no longer observed for $y=0.06$ [Inset of Fig. 1(b)]. Note also that T_C does not vary dramatically, being close to 125 K for $y=0.06$ and decreasing to 80 K for $y=0.10$. Correspondingly, the $\rho(T)$ curves (Fig. 2) are characterized by a maximum when doped with rhodium, indicating a tendency to a transition from an insulating paramagnetic state to a ferromagnetic metal like one, at decreasing temperature. Nevertheless, the value of the resistivity at low temperature remains high ($>5\times10^{-2}\,\Omega$ cm), so that most often the samples cannot be described even as bad metals, contrary to what is observed for chromium or ruthenium doping.[19–24] This is especially the case of the limit compounds $Pr_{0.65}Ca_{0.35}Mn_{1-y}Rh_yO_3$ [Fig. 2(a)] for which a bump in the resistivity is observed around 50 K for $y=0.05-0.10$, but the resistivity at low temperature, i.e., at 5 K, is still very high ($>10^3\,\Omega$ cm), though the ρ value at 5 K is too high to be measured in the undoped phase.[26] For larger calcium contents, the metallicity is significantly increased by Rh doping as shown for the $Pr_{0.5}Ca_{0.5}Mn_{1-y}Rh_yO_3$ series [Fig. 2(b)]. For the latter series, one indeed observes a peak shaped $\rho(T)$ curve whatever the Rh content, ranging from 2% to 10%, and the resistivity is decreased by several orders of magnitude with respect to the undoped material. The resistivity at low temperature (5 K) decreases indeed from $\geqslant 10^6\,\Omega$ cm for $y=0$ to $7\times10^{-2}\,\Omega$ cm for $y=0.04$ and increases again with y, reaching 30 Ω cm for $y=0.10$. Thus a transition from an insulating to a semimetallic or poorly metallic state is clearly observed for 4%–5% Rh. Note also that the transition temperature ($T_{peak}\sim 110$ K) follows the Curie temperature [Fig. 1(b)], increasing as y increases up to 4%, and then decreasing as y increases from 4% to 10%. These results will be discussed below in the picture of phase separation.[11]

For the electron rich region, the effect of Rh doping drops abruptly, as shown for $Pr_{0.4}Ca_{0.6}Mn_{1-y}Rh_yO_3$ (Fig. 3) which exhibits a much lower magnetic moment ranging from $0.25\mu_B$ for $y=0.05$ to $0.55\mu_B$ for $y=0.10$ [Fig. 3(a)] and remains insulating [Fig. 3(b)] whatever the rhodium content. Note that for $Pr_{0.2}Ca_{0.8}Mn_{1-y}Rh_yO_3$, practically no ferromagnetism is induced by Rh doping ($M<0.1\mu_B$) and the oxides remain insulating similarly to the pristine $y=0$ composition.[16]

As previously observed for the doping with magnetic cations,[20] the effect of Rh doping decreases with the average size of the A-site cation. For instance, the doping of $Sm_{0.5}Ca_{0.5}MnO_3$ with rhodium induces only small ferromag-

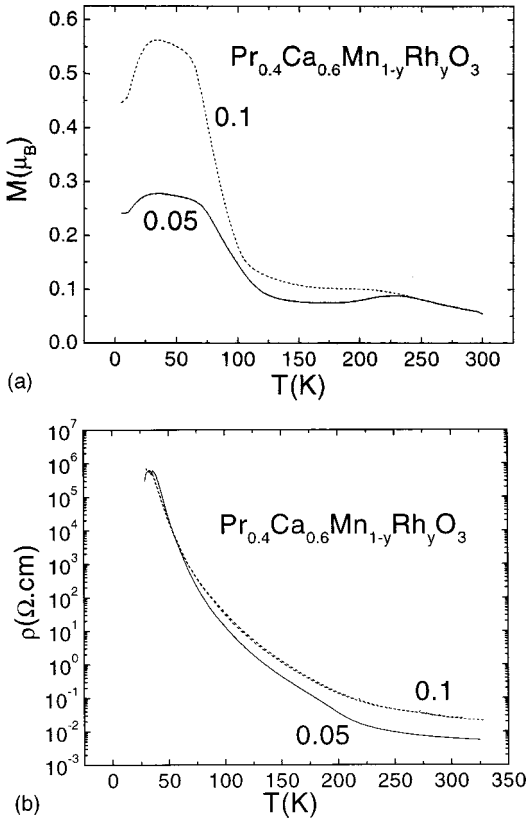

FIG. 3. $Pr_{0.4}Ca_{0.6}Mn_{1-y}Rh_yO_3$: (a) $M(T)$ and (b) $\rho(T)$ curves.

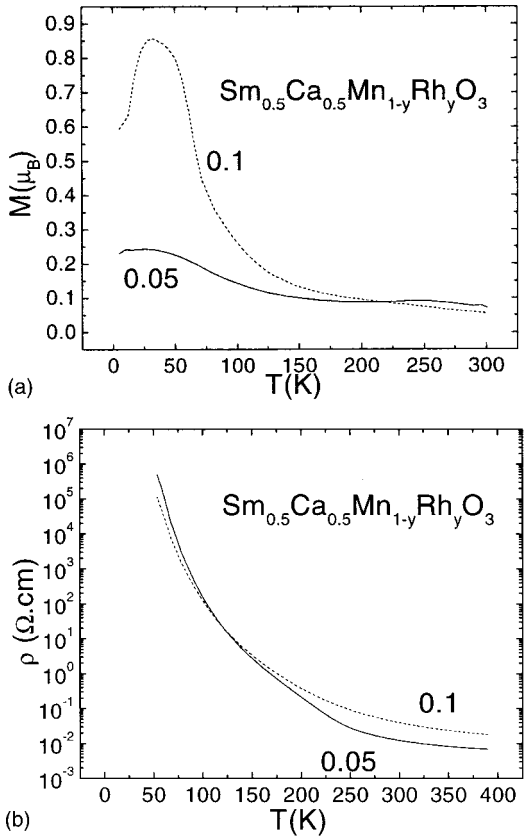

FIG. 4. $Sm_{0.5}Ca_{0.5}Mn_{1-y}Rh_yO_3$.: (a) $M(T)$ and (b) $\rho(T)$ curves.

netic components, $M=0.25\mu_B$ and $M=0.85\mu_B$ [Fig. 4(a)] for $y=0.05$ and 0.10, respectively, and, moreover, the materials remain insulating [Fig. 4(b)].

These results show that the doping of $Pr_{1-x}Ca_xMnO_3$ manganites with rhodium induces ferromagnetism and metallicity in a rather similar way as was found for chromium doping.[19,20] The most important effect of rhodium concerns its ability to induce ferromagnetism in the $Pr_{1-x}Ca_xMnO_3$ series with x ranging from 0.35 to 0.50, with magnetic moments very similar to those observed for Cr doping. Nevertheless, the Curie temperatures of the Rh-doped manganites are smaller than those of the Cr-doped compounds reaching maximum values of 120 K against 150 K for the Cr doped ones,[19,20] and the corresponding $M(T)$ curves are generally smoother, indicating that Rh is less effective in inducing ferromagnetism than Cr. This viewpoint is supported by the Rh-doped $Sm_{0.5}Ca_{0.5}MnO_3$ compounds which exhibit maximum magnetic moments at 5 K of $0.25-0.85\mu_B$ only, to be compared to the Cr-doped ones which reach maximum values of $1.2-2.0\mu_B$.[20] The less effective ability of Rh to induce ferromagnetism compared to Cr, is demonstrated by comparing the series $Pr_{0.4}Ca_{0.6}Mn_{1-y}Rh_yO_3$, which exhibit magnetic moments at 5 K of only $0.55\mu_B$, with the series $Pr_{0.4}Ca_{0.6}Mn_{1-y}Cr_yO_3$ for which magnetic moments of $2.5\mu_B$ are observed.[20] Finally Rh doping differs fundamentally from Cr doping by its significantly smaller efficiency to induce metallicity: we indeed observe for instance that the resistivity of the Rh-doped $Pr_{0.5}Ca_{0.5}MnO_3$ compounds is more than 1 order of magnitude larger than the corresponding Cr-doped samples.

The ability of rhodium to induce both ferromagnetism and a certain tendency to metallicity, ensures that CMR can be expected for the Rh-doped manganites. This is indeed observed for the $Pr_{0.65}Ca_{0.35}Mn_{1-y}Rh_yO_3$ series [Fig. 5(a)] which exhibits the highest resistivity ratios under 7 T at 50 K (ρ_{0T}/ρ_{7T} reaches 10^7 at 50 K) and for the $Pr_{0.5}Ca_{0.5}Mn_{1-y}Rh_yO_3$ series [Fig. 5(b)] which is characterized by a maximum value of the resistance ratio at T_C ($\rho_{0T}/\rho_{7T}\approx 10^2$). Note that the series $Pr_{0.4}Ca_{0.6}Mn_{1-y}Rh_yO_3$, exhibits CMR properties with resistivity ratios close to 10^5 at 50 K [Fig. 5(c)] though its ferromagnetic component is rather weak which indicates that these compositions lie close to the percolation threshold.

The Rh ability to progressively hinder the CO process at the benefit of the ferromagnetic metallic state as its content increases has been checked by ED as a function of temperature for $Pr_{0.5}Ca_{0.5}Mn_{0.95}Rh_{0.05}O_3$. At 92 K, the sample is made of the coexistence of small CO regions with ''nonordered'' ones. The latter are characterized by an orthorhombic structure (*Pbnma* space group) with ''$a_p\sqrt{2}\times 2a_p\times a_p\sqrt{2}$'' cell parameters where a_p is the primitive perovskite cell parameter. A typical ED pattern of such a nonordered area is given in Fig. 6(a); it is similar to the room temperature one. In contrast, the CO regions observed at 92 K exhibit ED patterns with extra peaks in incommensurate positions [Fig. 6(b)]. This system of satellites is characteristic of the CO state, with a modulation vector qa^*, so that a subcell $(1/q)a_p\sqrt{2}\times 2a_p\times a_p\sqrt{2}$ is obtained with an average q value close to 0.46. Note that the coexistence of ordered and

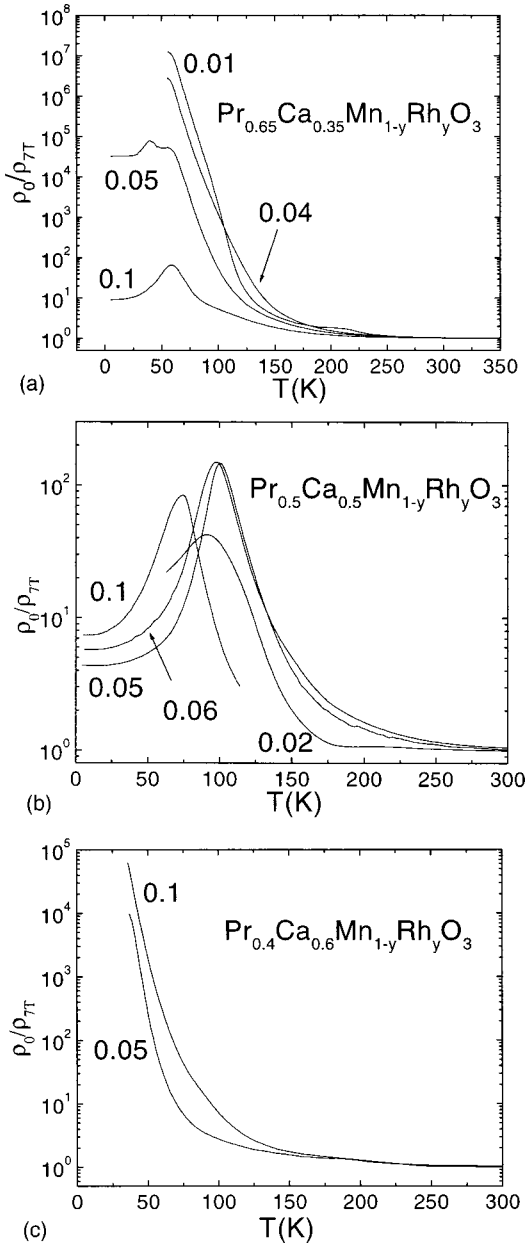

FIG. 5. T dependent resistivity ratios ρ_0/ρ_{7T} obtained by dividing the resistivity in the absence of magnetic field (ρ_0) by the resistivity measured in the $7T(\rho_{7T})$. Both sets of data, $\rho_0(T)$ and $\rho_{7T}(T)$ are collected in cooling mode: (a) $Pr_{0.65}Ca_{0.35}Mn_{1-y}Rh_yO_3$; (b) $Pr_{0.5}Ca_{0.5}Mn_{1-y}Rh_yO_3$; (c) $Pr_{0.4}Ca_{0.6}Mn_{1-y}Rh_yO_3$.

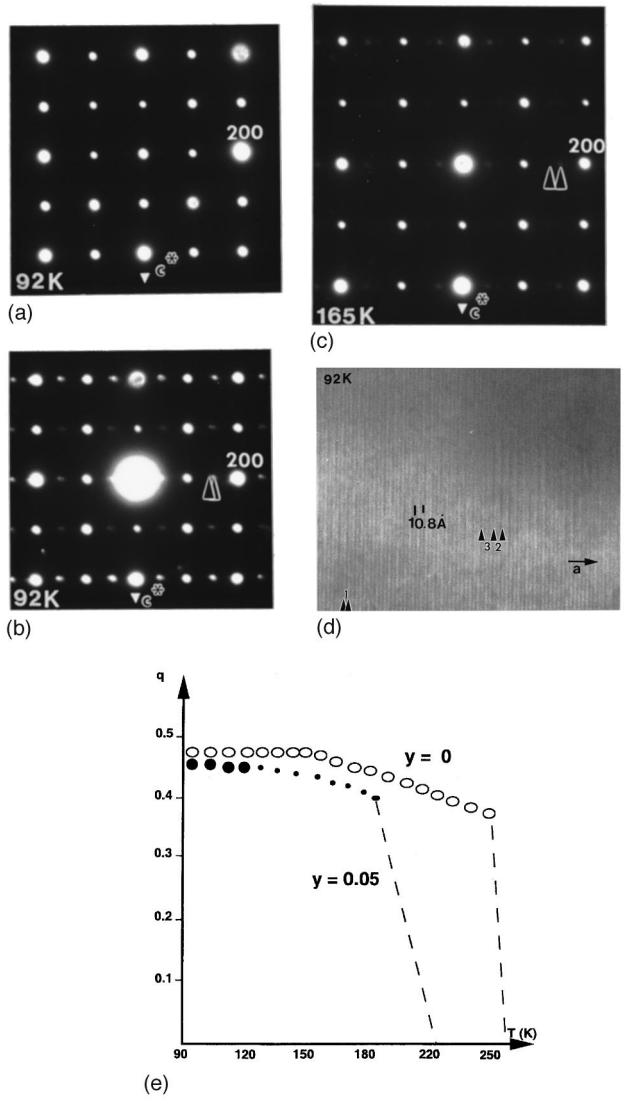

FIG. 6. [010] orientation of the $Pr_{0.5}Ca_{0.5}Mn_{0.95}Rh_{0.05}O_3$ crystals: (a) ED pattern at 92 K for a nonordered area and (b) ED pattern at 92 K for a CO area; (c) ED pattern at 165 K for the same CO area; (d) [010] lattice image recorded at 92 K. In the CO areas the fringe spacing is $\mathbf{n}a_p\sqrt{2}$, with $\mathbf{n}=2$ and 3 (black numbering) and $a_p\sqrt{2}$ in the *Pnma*-type areas; (e) T dependence of the modulation vector q for $Pr_{0.5}Ca_{0.5}MnO_3$ and for the remaining CO regions of $Pr_{0.5}Ca_{0.5}Mn_{0.95}Rh_{0.05}O_3$. The size of the symbols reflects the intensity of the satellites.

nonordered domains was also observed in the $Pr_{0.5}Ca_{0.5}Mn_{0.95}Cr_{0.05}O_3$,[27] but with a lower modulation vector ($q=0.39$). The lattice images recorded at 92 K confirm that the sample is made of CO domains, a few tens of nanometers wide, in a nonordered *Pnma*-type matrix. One example is given in Fig. 6(d). The contrast consists of bright and less bright fringes. In the small CO areas, the local periodicity is $\mathbf{n}a_p\sqrt{2}$, with $\mathbf{n}=2$ and 3 (see in the middle part of the image, between small black arrows). In the rest of the grain, the distance between two fringes of equal intensity is $a_p\sqrt{2}$, ($\mathbf{n}=1$), in agreement with the cell parameter of the nonordered structure (lower part of the image).

By warming the samples, the q value remains roughly constant in the range 92–120 K [Fig. 6(e)]. Above 125 K, the intensity of the satellites abruptly decreases whereas concomitantly the q value smoothly decreases. This is illustrated in Fig. 6(c), recorded at 165 K [same area as Fig. 6(b)]. At 200 K, the q value is close to 0.4 and the satellites are scarcely visible. Between 200 and 230 K, there are no nodes but only diffuse streaks along a^*, and above 230 K they are no longer detectable. These results indicate that T_{CO} is depressed in the doped $Pr_{0.5}Ca_{0.5}Mn_{0.95}Rh_{0.05}O_3$, in comparison with $T_{CO}=250$ K for the pristine $Pr_{0.5}Ca_{0.5}MnO_3$ compound.

Accordingly, the field dependent magnetization $M(H)$ curve registered at 5 K for $y=0.05$ exhibits a ferromagnetic behavior with a saturation at $3\mu_B$/f.u., i.e., close to the expected moment ($\sim 3.5\mu_B$), which is very different from the

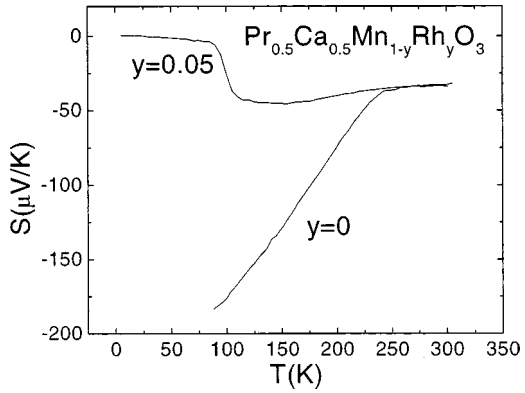

FIG. 7. T dependence of the thermopower S for the compounds $Pr_{0.5}Ca_{0.5}MnO_3$ ($y=0$) and $Pr_{0.5}Ca_{0.5}Mn_{0.95}Rh_{0.05}O_3$ ($y=0.05$).

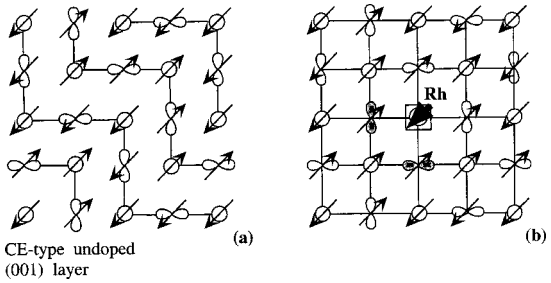

FIG. 8. (a) Orbital, charge and spin ordering of the CE-type structure. (b) Creation of ferromagnetic regions by Rh^{4+} doping.

low M values obtained for the CO–AFM $y=0.00$ sample [Fig. 1(b)].

Another proof of the gradual disappearance of charge ordering induced by Rh doping is given by thermopower measurements. These measurements were performed on the sample $Pr_{0.5}Ca_{0.5}Mn_{0.95}Rh_{0.05}O_3$. Figure 7 presents the results obtained as the sample was cooled from 320 to 5 K under zero field. They are compared to the results obtained for the undoped sample $Pr_{0.5}Ca_{0.5}MnO_3$ ($y=0$). As previously described in Ref. 28, the charge ordering transition in $Pr_{0.5}Ca_{0.5}MnO_3$ at $T_{CO}\approx 250$ K is associated with a steep decrease of the thermopower leading to large negative values at low temperatures. Doping the compound with 5% of Rh strongly modifies thermopower. The steep decrease of $S(T)$ is changed into a slowly decreasing value of S as T decreases. At $T\approx 90$ K, as the sample enters the ferromagnetic and ''metallic'' state as shown in Figs. 1(b) and 2(b), the absolute value of thermopower goes back to very small values, characteristic of a ''metal.'' This strong decrease of the absolute value of S in the high temperature insulating phase of the doped compound ($90\,\mathrm{K}<T<T_{CO}$) shows that long-range ferromagnetic ordering has been efficiently stabilized by Rh doping.

In order to explain the role of rhodium in the magnetic and transport properties of these doped manganites, there are several aspects to consider. They include the electronic configuration of rhodium and the coupling to its environment. Also one needs to figure out why a (bad) metallic behavior sets in and the reason for the observed ferromagnetism. We now proceed to these considerations. Concerning first the electronic configurations of rhodium, we may consider, according to previous studies,[29] that rhodium is either trivalent or tetravalent. The substitution of Rh^{3+} for Mn^{3+} in those oxides would not introduce any ferromagnetism, nor metallicity since the $(t_{2g})^6 e_g^0$ configuration of this species would lead to $S=0$ as shown previously for d° cations (Mg^{2+}, Al^{3+}, Ti^{4+}, Nb^{5+}).[30] The doping of these oxides with Rh^{4+}, with the $(t_{2g})^5$ configurations is on the other hand susceptible to introducing ferromagnetism and metallicity similar to Rh^{4+}, which is in the $(t_{2g})^4$ configuration.[21–24] Let us indeed consider the Rh^{4+} doping of the charge ordered charge exchange (CE)-type structure of $Pr_{0.5}Ca_{0.5}MnO_3$ [see projected two-dimensionaly structure Fig. 8(a)], in an otherwise undisturbed charge-ordered state, in a static picture. This structure consists of FM zig-zag chains of Mn^{3+}/Mn^{4+} cations, the coupling between chains being antiferromagnetic. In other words, one Mn atom is primarily coupled to two of its Mn neighbors through e_g electrons, and weakly coupled to the other four through t_{2g} electrons. One should first notice that the ionic radius of Rh^{4+}(0.6 Å) is substantially larger than that of Mn^{4+}(0.53 Å), but similar to Mn^{3+}(0.64 Å). Therefore the Rh^{4+} ions should be sitting at the center of the MnO_6 octahedron in contrast to the off-centered location of Mn^{4+}.[31] As a result, one expects that the coupling of Rh^{4+} to its neighbors is going to be more symmetrical than it is the case for Mn^{4+}, thus leading to a local suppression of the charge ordering of the CE-type structure. As the rhodium content increases, the nonordered regions will percolate, yielding a metallic behavior.

Having explained the role of rhodium substitution in establishing a metallic behavior, we turn to the magnetism. In this context one may expect that the larger Rh^{4+} would ''push away'' surrounding oxygen as a result of which the orbitals of Mn^{3+} surrounding Rh^{4+} will all be directed away from it [see Fig. 8(b)]. One immediately sees that, according to Goodenough–Kanamori rules, the spins of these flipped Mn^{3+} ions would be reversed, creating small ferromagnetic clusters and establishing conducting ''bridges'' between neighboring parallel zigzag chains which, before introducing Rh^{4+}, were separated by the antiparallel ones. This may be a factor contributing to the establishing of the FM state by rhodium doping.

There exists however yet another, and probably more important mechanism. Notably, there may occur valence fluctuations of the type $Mn^{3+}+Rh^{4+}\leftrightarrow Mn^{4+}+Rh^{3+}$. Note that these valence fluctuations would most probably occur via hopping of e_g electrons, as a result of which the $Rh^{3+}(d^6)$ will be in an excited intermediate spin state ($t_{2g}^5 e_g^1$), similar to such state in Co^{3+}.[32] They can effectively destroy charge ordering and provide an efficient mechanism for the ferromagnetism and metallic conductivity similar to the conventional double exchange (this mechanism is analogous to the one responsible for the FM behavior of the double perovskites Sr_2FeMoO_6).[33] This process is efficient for underdoped systems, when we have many Mn^{3+} ions. However for over doped system ($x\geqslant 0.6$), Rh^{4+} is predominantly surrounded by Mn^{4+} ions, so that this mechanism becomes less and less efficient, in contrast to Ru doping

where similar valence fluctuations are $Mn^{4+}+Ru^{4+} \leftrightarrow Mn^{3+}+Ru^{5+}$.

IV. CONCLUSION

Anomalous ferromagnetic phase induced by rhodium substitution in charge-ordered manganites $Pr_{1-x}Ca_xMnO_3$ has been discovered. It extends from $x=0.35$ to $x=0.5$. With Curie temperatures around 100 K it is found that Rh doping is less efficient than Cr or Ru doping. Nevertheless, the induced phase separation is responsible for the observed CMR properties. These properties are understood as following from the collapse of the charge ordering transition as probed by the dramatic change in the thermopower.

ACKNOWLEDGMENT

The authors gratefully acknowledge C. Martin for interesting discussions.

[1] P. H. Woodward, D. E. Cox, T. Vogt, C. N. R. Rao, and A. K. Cheetham, Chem. Mater. **11**, 3528 (1999).
[2] C. H. Shen and S. W. Cheong, Phys. Rev. Lett. **76**, 4042 (1996).
[3] F. Damay, Z. Jirak, M. Hervieu, C. Martin, A. Maignan, B. Raveau, G. André, and F. Bourée, J. Magn. Magn. Mater. **190**, 221 (1998).
[4] M. Hervieu, A. Barnabé, C. Martin, A. Maignan, F. Damay, and B. Raveau, Eur. Phys. J. B **8**, 31 (1999); J. Mater. Chem. **8**, 1405 (1998).
[5] Z. Jirak, S. Krupicka, Z. Simsa, M. Dlouha, and S. Vratislav, J. Magn. Magn. Mater. **53**, 153 (1985).
[6] C. H. Chen, S. W. Cheong, and H. Y. Hwang, J. Appl. Phys. **81**, 4326 (1997).
[7] P. Schiffer, A. P. Ramirez, W. Bao, and S. W. Cheong, Phys. Rev. Lett. **75**, 3336 (1995).
[8] P. G. Radaelli, D. E. Cox, M. Marezio, S. W. Cheong, P. Schiffer, and A. P. Ramirez, Phys. Rev. Lett. **75**, 4488 (1995).
[9] G. Allodi, R. De Renzi, G. Gvidi, F. Licci, and M. W. Piepper, Phys. Rev. B **56**, 6036 (1997).
[10] A. Moreo, S. Yunoki, and E. Dagotto, Science **283**, 2034 (1999).
[11] D. Khomskii, Physica B **280**, 325 (2000).
[12] M. Yu, Kagan, K. I. Kugel, and D. Khomskii, cond-mat/0001245.
[13] G. Allodi, R. De Renzi, F. Licciand, and M. W. Piepper, Phys. Rev. Lett. **81**, 4736 (1998).
[14] N. Kumar and C. N. R. Rao, J. Solid State Chem. **129**, 363 (1997).
[15] A. Barnabé, M. Hervieu, C. Martin, A. Maignan, and B. Raveau, J. Appl. Phys. **84**, 5506 (1998).
[16] C. Martin, A. Maignan, M. Hervieu, and B. Raveau, Phys. Rev. B **60**, 12191 (2000).
[17] F. Damay, C. Martin, A. Maignan, M. Hervieu, Z. Jirak, G. André, and F. Bourée, Chem. Mater. **11**, 536 (1999).
[18] A. Maignan, F. Damay, C. Martin, and B. Raveau, Mater. Res. Bull. **32**, 965 (1997).
[19] B. Raveau, A. Maignan, and C. Martin, J. Solid State Chem. **130**, 162 (1997).
[20] A. Barnabé, A. Maignan, M. Hervieu, C. Martin, and B. Raveau, Appl. Phys. Lett. **71**, 3907 (1997); Eru. Phys. J. B **1**, 145 (1998).
[21] P. V. Vanitha, A. Arulraj, A. R. Raju, and C. N. R. Rao, C. R. Acad. Sci. **IIc**, 595 (1999).
[22] B. Raveau, A. Maignan, C. Martin, R. Mahendiran, and M. Hervieu, J. Solid State Chem. **151**, 330 (2000).
[23] C. Martin, A. Maignan, M. Hervieu, B. Raveau, and J. Hejtmanek, Eur. J. Phys. **16**, 469 (2000).
[24] C. Martin, A. Maignan, M. Hervieu, C. Autret, B. Raveau, and D. I. Khomskii, Phys. Rev. B (to be published).
[25] A. Maignan, C. Martin, M. Hervieu, B. Raveau, and J. Hejtmanek, J. Appl. Phys. **89**, 2232 (2001).
[26] Y. Tomioka, A. Asamitsu, H. Kuwahara, Y. Moritomo, and Y. Tokura, Phys. Rev. B **53**, R1689 (1996).
[27] M. Hervieu, C. Martin, A. Barnabé, A. Maignan, R. Mahendiran, and V. Hardy, Solid State Sci. (in press).
[28] J. Hejtmanek, Z. Jirak, Z. Arnold, M. Marysko, S. Krupicka, C. Martin, and F. Damay, J. Appl. Phys. **83**, 7204 (1998).
[29] D. Y. Jung and G. Demazeau, Solid State Commun. **94**, 963 (1995); M. Zakhour, PhD thesis, University of Bordeaux I, July 2000.
[30] F. Damay, C. Martin, A. Maignan, and B. Raveau, J. Magn. Magn. Mater. **183**, 143 (1998).
[31] Z. Jirak, F. Damay, M. Hervieu, C. Martin, B. Raveau, G. André, and F. Bourée, Phys. Rev. B **61**, 1181 (2000).
[32] M. A. Senaris-Rodriguez and J. B. Goodenough, J. Solid State Chem. **118**, 323 (1995).
[33] K. I. Kobayashi, T. Kimura, H. Sawada, K. Terakura, and Y. Tokura, Nature (London) **395**, 677 (1998); D. Sarma *et al.*, Phys. Rev. Lett. **85**, 2549 (2000).